

Ultrafast Phenomena V

Proceedings of the Fifth OSA Topical Meeting
Snowmass, Colorado, June 16–19, 1986

Editors: G.R. Fleming and A.E. Siegman

With 427 Figures

Springer-Verlag Berlin Heidelberg New York
London Paris Tokyo

Contents

Part I	Mode Locking and Ultrashort Pulse Generation	
<hr/>		
Passive and Hybrid Femtosecond Operation of a Linear Astigmatism Compensated Dye Laser By J.-C. Diels, N. Jamasbi, and L. Sarger (With 1 Figure)		2
Generation of 55-fs Pulses and Variable Spectral Windowing in a Linear-Cavity Synchronously Pumped cw Dye Laser By M.D. Dawson, T.F. Boggess, D.W. Garvey, and A.L. Smirl (With 4 Figures)		5
Cavity-Mirror Dispersion Dependence of Pulse Duration Generated from a Simple CPM Laser: An Experimental Study By M. Yamashita, K. Torizuka, T. Sato, and M. Ishikawa (With 2 Figures)		8
Femtosecond Pulse Generation from Passively Mode Locked Continuous Wave Dye Lasers 550–700 nm By P.M.W. French and J.R. Taylor (With 3 Figures)		11
Stabilisation of a CPM Dye Laser Synchronously Pumped by a Frequency Doubled ML YAG Laser By J. Chesnoy and L. Fini (With 3 Figures)		14
Fluctuations and Chirp in Colliding-Pulse Mode-Locked Dye Lasers. By D. Kühlke, T. Bonkhofer, U. Herpers, and D. von der Linde (With 2 Figures)		17
Experimental Observation of High Order Solitons in a Colliding Pulse Mode-Locked Laser By F. Salin, P. Grangier, G. Roger, and A. Brun (With 4 Figures)		20
Advances in the Theory of Mode-Locking by Synchronous Pumping. By G.H.C. New and J.M. Catherall (With 3 Figures) ...		24
Collective Modes - An Analytical Model for Active Mode Locking in the Transient Case By P. Aechtner, P. Heinz, and A. Laubereau (With 2 Figures)		27

Generation of Picosecond Pulses from a Continuous Wave Neodymium:Phosphate Glass Laser By L. Yan, J.D. Ling, P.-T. Ho, and C.H. Lee (With 3 Figures)	30
--	----

Part II Ultrafast Optical Generation and Measurement Techniques

Fourier Transform Picosecond Pulse Shaping and Spectral Phase Measurement in a Grating Pulse-Compressor. By J.P. Heritage, A.M. Weiner, and R.N. Thurston (With 4 Figures)	34
Picosecond Pulse Amplification Using Pulse Compression Techniques. By D. Strickland, P. Maine, M. Bouvier, S. Williamson, and G. Mourou (With 4 Figures)	38
New Optical Design for a Jet Amplifier. By O. Seddiki, A. Goddi, R. Mounet, J.-F. Morhange, and C. Hirlimann (With 2 Figures) ...	43
Fiber Raman Amplification Soliton Laser (FRASL) By M.N. Islam, L.F. Mollenauer, and R.H. Stolen (With 4 Figures)	46
Dispersion Compensated Fiber Raman Oscillator By J.D. Kafka, D.F. Head, and T. Baer (With 2 Figures)	51
80-fs Soliton-like Pulses from an Optical Nonlinear Fiber Resonator. By B. Zysset, P. Beaud, W. Hodel, and H.P. Weber (With 4 Figures)	54
The Stabilized Soliton Laser By F.M. Mitschke and L.F. Mollenauer (With 4 Figures)	58
The Soliton Self Frequency Shift. By F.M. Mitschke, L.F. Mollenauer, and J.P. Gordon (With 2 Figures)	62
Solitons at the Zero Dispersion Wavelength of Single-Mode Fibers By P.K.A. Wai, C.R. Menyuk, H.H. Chen, and Y.C. Lee (With 1 Figure)	65
Active Mode-Locking of an InGaAsP Optical-Fiber Ring Laser By G. Eisenstein, R.M. Jopson, M.S. Whalen, K.L. Hall, and G. Raybon (With 4 Figures)	68
Femtosecond Resolved Fluorescence By W. Rudolph and J.-C. Diels (With 2 Figures)	71
Parametric Amplification Sampling Spectroscopy (PASS): A New Technique for Resolving Near-Infrared Luminescence on a Subpicosecond Time Scale. By D. Hulin, A. Migus, A. Antonetti, I. Ledoux, J. Badan, and J. Zyss (With 3 Figures)	75

Measurement of Optical Phase with Subpicosecond Resolution by Time Domain Interferometry. By J.E. Rothenberg (With 6 Figures)	78
Real Time Picosecond Optical Oscilloscope By J.A. Valdmanis (With 8 Figures)	82
Beam Overlap for Long Delay Lines Using Active Feedback By C. Doland, W.B. Jackson, and A. Andersson (With 3 Figures) .	86
Ultrashort Dye Laser Pulses Using the Sweeping Oscillator Method. By Y.H. Meyer, M.M. Martin, E. Br��h��ret, and O. Benoit d'Azy (With 4 Figures)	89
An Investigation on Ultrashort Light Pulse Generation by Travelling-Wave Amplified Spontaneous Emission By W. Lee, C. Ning, Z. Huang, and W. Wang (With 5 Figures) ...	92

Part III Electrooptic Sampling Techniques

Electrooptic Sampling of Gallium Arsenide Integrated Circuits By K.J. Weingarten, M.J.W. Rodwell, J.L. Freeman, S.K. Diamond, and D.M. Bloom (With 6 Figures)	98
Picosecond Characterization of Ultrafast Phenomena: New Devices and New Techniques. By D.R. Dykaar, R. Sobolewski, J.F. Whitaker, T.Y. Hsiang, G.A. Mourou, M.A. Hollis, B.J. Clifton, K.B. Nichols, C.O. Bozler, and R.A. Murphy (With 4 Figures)	103
Precise Measurement of Signal Propagation Characteristics in GaAs Integrated Circuits by Picosecond Electro-Optic Sampling By R.K. Jain, X.-C. Zhang, M.G. Ressler, and T.J. Pier (With 2 Figures)	107
Propagation of Ultrashort Electrical Pulses on Superconducting Transmission Lines By I.N. Duling III, C.-C. Chi, W.J. Gallagher, D. Grischkowsky, N.J. Halas, M.B. Ketchen, and A.W. Kleinsasser (With 4 Figures)	110
High Repetition Rate Electro-Optic Sampling with an Injection Laser. By A.J. Taylor, R.S. Tucker, J.M. Wiesenfeld, G. Eisenstein, and C.A. Burrus (With 5 Figures)	114
Picosecond Optoelectronic Sampling of Electrical Waveforms Produced by an Optically Excited Field Effect Transistor By D.E. Cooper and S.C. Moss (With 1 Figure)	117

Picosecond Electrical Pulses in Microelectronics. By P.G. May, G.P. Li, J.-M. Halbout, M.B. Ketchen, C.-C. Chi, M. Scheuermann, I.N. Duling III, D. Grischkowsky, and M. Smyth (With 3 Figures) .	120
High Speed Circuit Measurements Using Photoemission Sampling By J. Bokor, A.M. Johnson, R.H. Storz, and W.M. Simpson (With 2 Figures)	123
Photoemissive Sampling of Picosecond Electrical Waveforms By A.M. Weiner, R.B. Marcus, P.S.D. Lin, and J.H. Abeles (With 5 Figures)	127
Nonlinear Responses of Picosecond Photodetectors to Photogenerated Carriers By T.F. Carruthers and J.F. Weller (With 3 Figures)	131
Direct Generation of Picosecond to Subpicosecond Optical Pulses Using Electrooptic Modulation Methods By T. Kobayashi, A. Morimoto, T. Fujita, K. Amano, T. Uemura, and T. Sueta (With 6 Figures)	134
Elimination of Dynamic Flash in a Picosecond Streak Image Tube By Huanwen Zhang (With 1 Figure)	137

Part IV Nonlinear Optics and Continuum Generation

Parametric Chirp Reversal and Enhancement: Application in Femtosecond Optics. By A. Piskarskas, D. Podenas, A. Stabinis, A. Umbrasas, A. Varanavichius, A. Yankauskas, and G. Yonushauskas (With 7 Figures)	142
Supercontinuum Generation in Gases: A High Order Nonlinear Optics Phenomenon. By P.B. Corkum, C. Rolland, and T. Srinivasan-Rao (With 3 Figures)	149
New Excitation and Probe Continuum Sources for Subpicosecond Absorption Spectroscopy By J.H. Glownia, J. Misewich, and P.P. Sorokin (With 2 Figures) .	153
Induced Phase Modulation and Spectral Broadening of a Weak 530-nm Picosecond Pulse by an Intense 1060-nm Picosecond Pulse in Glass. By R.R. Alfano, Q.X. Li, T. Jimbo, J.T. Manassah, and P.P. Ho (With 2 Figures)	157
The Observation of Chirped Stimulated Raman Scattered Light in Fibers. By A.M. Johnson, R.H. Stolen, and W.M. Simpson (With 3 Figures)	160

Observation of 7.2-THz Beats Between the D-Lines of Atomic Rb By J.E. Golub and T.W. Mossberg (With 1 Figure)	164
Coherent Multiphoton Resonant Interaction and Harmonic Generation. By A. Mukherjee, N. Mukherjee, J.-C. Diels, and G. Arzumanyan (With 4 Figures)	166
Ultrafast Chaos from Semiconductor Lasers. By Y. Cho, T. Umeda, I. Jun Cha, M. Koishi, and M. Miwa (With 5 Figures) .	169

**Part V Applications to Semiconductors, Quantum Wells, and
 Solid State Physics**

Thermodynamics and Kinetics of Melting, Evaporation and Crystallization, Induced by Picosecond Pulsed Laser Irradiation By F. Spaepen (With 1 Figure)	174
Investigation of Nonthermal Population Distributions with 10-fs Optical Pulses. By C.V. Shank, R.L. Fork, C.H. Brito Cruz, and W. Knox (With 3 Figures)	179
Superheating During Ultrafast Laser Heating of Semiconductors By D. von der Linde, N. Fabricius, B. Danielzik, and P. Hermes (With 4 Figures)	182
Non-equilibrium Carriers in GaAs: Secondary Emission During the First Two Picoseconds By J.A. Kash and J.C. Tsang (With 5 Figures)	188
Ultrafast Carrier Dynamics in GaAs and $Al_xGa_{1-x}As$ By W.Z. Lin, J.G. Fujimoto, E.P. Ippen, and R.A. Logan (With 4 Figures)	193
Subpicosecond Optical Non-linearities in GaAs Multiple-Quantum- Well Structures. By D. Hulin, A. Antonetti, A. Migus, A. Mysyrowicz, H.M. Gibbs, N. Peyghambarian, W.T. Masselink, and H. Morkoç (With 5 Figures)	197
Picosecond Relaxation of Nonthermal Wannier Excitons in GaAs By L. Schultheis, J. Kuhl, A. Honold, and C.W. Tu (With 1 Figure)	201
Picosecond Observation of the Photorefractive Effect in GaAs By A.L. Smirl, G.C. Valley, M.B. Klein, K. Bohnert, and T.F. Boggess (With 2 Figures)	203

Time-Resolved Photoluminescence Measurements in $\text{Al}_x\text{Ga}_{1-x}\text{As}$ Under Intense Picosecond Excitation By K. Bohnert, H. Kalt, D.P. Norwood, T.F. Boggess, A.L. Smirl, and R.Y. Loo (With 2 Figures)	207
Picosecond Excite-Probe and Transient Grating Studies of $\text{Ga}_x\text{In}_{1-x}\text{As}_y\text{P}_{1-y}$. By R.J. Manning, A. Miller, A.M. Fox, and J.H. Marsh (With 2 Figures)	210
Ultrafast Dynamics in GaAlAs Diode Laser Amplifiers By M.S. Stix, M.P. Kesler, and E.P. Ippen (With 8 Figures)	213
Electronic Energy Relaxation and Localization in Two II-VI Compound Semiconductor Quantum Well Structures By Y. Hefetz, W.C. Goltsov, D. Lee, and A.V. Nurmikko (With 6 Figures)	218
Transient Raman Scattering in Multiple Quantum Well Structures By D.Y. Oberli, D.R. Wake, M.V. Klein, J. Klem, and H. Morkoç (With 2 Figures)	223
Fast Energy Relaxation of Hot Electrons in Bulk GaAs and Multi- Quantum Wells. By C.H. Yang and S.A. Lyon (With 2 Figures) ...	227
Picosecond Photoluminescence and Energy-Loss Rates in GaAs Quantum Wells Under High-Density Excitation By T. Kobayashi, H. Uchiki, Y. Arakawa, and H. Sakaki (With 4 Figures)	231
Broad Tuning of the Photoluminescence Energy and Lifetime by the Quantum-Confined Stark Effect. By H.-J. Polland, L. Schultheis, J. Kuhl, E.O. Göbel, and C.W. Tu (With 2 Figures)	234
Auger Heating of Silicon-on-Sapphire by Femtosecond Optical Pulses. By M.C. Downer and C.V. Shank (With 2 Figures)	238
The Origin of Picosecond Photoinduced Absorption Decays in Hydrogenated Amorphous Silicon By W.B. Jackson, C. Doland, and C.C. Tsai (With 2 Figures)	242
Picosecond Decay of Photoinduced Absorption in Hydrogenated Amorphous Silicon By D.M. Roberts and T.L. Gustafson (With 2 Figures)	245
Femtosecond Spectroscopy of Hot Carriers in Germanium By P.M. Fauchet, D. Hulin, G. Hamoniaux, A. Orszag, J. Kolodzey, and S. Wagner (With 3 Figures)	248

Spin Dephasing Kinetics of Free Carriers in Alloy Semimagnetic Semiconductors $Cd_{1-x}Mn_xSe$ by One and Two Photon Excitation By M.R. Junnarkar and R.R. Alfano (With 1 Figure)	251
Detection of Higher Order Fourier Components of Index Gratings in Picosecond Transient Grating Experiments By E.O. Göbel and H. Saito (With 3 Figures)	254
Transient Thermoreflectance Studies of Thermal Transport in Compositionally Modulated Metal Films. By G.L. Eesley, C.A. Paddock, and B.M. Clemens (With 2 Figures)	257
Femtosecond Studies of Nonequilibrium Electronic Processes in Metals. By R.W. Schoenlein, W.Z. Lin, J.G. Fujimoto, and G.L. Eesley (With 4 Figures)	260
Time-Resolved Observation of Electron-Phonon Relaxation During Femtosecond Laser Heating of Copper. By H. Elsayed-Ali, M. Pessot, T. Norris, and G. Mourou (With 2 Figures)	264
Femtosecond Carrier Relaxation in Semiconductor-Doped Glasses By M.C. Nuss, W. Zinth, and W. Kaiser (With 2 Figures)	267
Femtosecond Dynamics of Electron-Hole Plasma in Semiconductor Microcrystallite Doped Glass. By G.R. Olbright, B.D. Fluegel, S.W. Koch, and N. Peyghambarian (With 2 Figures)	270
High-Contrast Ultrafast Phase Conjugation in Semiconductor-Doped Glass. By D. Cotter (With 3 Figures)	274
Femtosecond Vibrational Relaxation of the $F\frac{1}{2}$ Center in LiF By W.H. Knox, L.F. Mollenauer, and R.L. Fork (With 2 Figures) .	277
Determination of the Rapid Quenching Rates of Excited State F-Centers by OH^- Defects in KCl. By Du-Jeon Jang, T.C. Corcoran, M.A. El-Sayed, L. Gomes, and F. Luty (With 4 Figures)	280
Propagation of Coherent Phonon Polaritons in $LiTaO_3$ Measured by FIR-Cherenkov-Pulses By M.C. Nuss and D.H. Auston (With 3 Figures)	284

Part VI Chemical Reaction Dynamics

Cages, Crossings and Correlations – Theoretical Perspectives on Solution Reaction Dynamics. By J.T. Hynes	288
---	-----

Polarity Dependent Barriers and the Photoisomerization Dynamics of Polar Molecules in Solution. By J.M. Hicks, M.T. Vandersall, E.V. Sitzmann, and K.B. Eisenthal (With 3 Figures)	293
Dynamic Solvent Effects on Small Barrier Isomerizations By P.F. Barbara and V. Nagarajan (With 3 Figures)	299
Solvation Dynamics in Polar Liquids: Experiment and Simulation By M. Maroncelli, E.W. Castner, Jr., S.P. Webb, and G.R. Fleming (With 4 Figures)	303
Femtosecond Study of Electron Localization and Solvation in Pure Water. By Y. Gauduel, J.L. Martin, A. Migus, N. Yamada, and A. Antonetti (With 2 Figures)	308
Time-Dependent Fluorescence Shift in Alcoholic Solvents: A Non-Debye Behaviour Related to Hydrogen Bonds By C. Rullière, A. Declémy, and Ph. Kottis (With 4 Figures)	312
Picosecond Dynamics of Proton-Anion Ion Pair Geminate Recombination. By D. Huppert and E. Pines (With 1 Figure)	315
Excited State Proton Transfer in Matrix Isolated Water and Methanol Complexes of 2-Hydroxy-4,5-benzotropone and 3-Hydroxyflavone By D.F. Kelley and G.A. Brucker (With 2 Figures)	319
Detection of the Inverted Region in Photo-induced Intramolecular Electron Transfer. By R.J. Harrison, G.S. Beddard, J.A. Cowan, and J.K.M. Sanders (With 2 Figures)	322
Ultrafast Studies Designed to Test the Fundamental Statistical Assumptions Underlying Chemical Reactivity in Liquids By C.B. Harris, J.K. Brown, M.E. Paige, D.E. Smith, and D.J. Russell (With 4 Figures)	326
Geminate Recombination and Relaxation of Condensed Phase Molecular Halogens By D.F. Kelley and N.A. Abul Haj (With 1 Figure)	330
Fast Photochemical Processes of Aromatic Nitro Compounds in Solution. By B.B. Craig, S.K. Chattopadhyay, and J.C. Mialocq (With 4 Figures)	334
Cage Recombination and Unimolecular β -Scission Reactions of Sulfur Centered Free Radicals By T.W. Scott and S.N. Liu (With 3 Figures)	338

The Influence of Friction and Deuteration on Stilbene Isomerization. By S.H. Courtney, M.W. Balk, S. Canonica, S.K. Kim, and G.R. Fleming (With 3 Figures)	341
Kramers-Hubbard Approach to the Solvent Dependence of Isomerization. By M. Lee and R.M. Hochstrasser (With 3 Figures)	344
Photoisomerization Studies of Substituted Stilbenes: 4,4'-Dihydroxystilbene and 4,4'-Dimethoxystilbene By D.M. Zeglinski and D.H. Waldeck (With 2 Figures)	347
Picosecond Studies of Barrierless Torsional Diffusion By D. Ben-Amotz and C.B. Harris (With 2 Figures)	350
Time-Resolved Fluorescence Spectra of Ethidium Bromide By J.H. Sommer, T.M. Nordlund, M. McGuire, and G. McLendon (With 3 Figures)	353
Picosecond and Femtosecond Molecular Beam Chemistry: Coherence and Fragment Recoil Dynamics By A.H. Zewail (With 4 Figures)	356
Picosecond Laser Study of the Collisionless UV Photodissociation of Energetic Materials By J.-C. Mialocq and J.C. Stephenson (With 3 Figures)	362
Experimental Study of Harmonic Generation with Picosecond 248 nm Radiation. By T.S. Luk, A. McPherson, H. Jara, U. Johann, I.A. McIntyre, A.P. Schwarzenbach, K. Boyer, and C.K. Rhodes (With 2 Figures)	366
Time-Resolved Measurement of Laser-Induced Desorption of a Molecular Monolayer. By G. Arjavalingam, T.F. Heinz, and J.H. Glowonia (With 1 Figure)	370

Part VII Dynamics of Biological Processes

Picosecond Electron Transfer and Stimulated Emission in Reaction Centers of <i>Rhodobacter sphaeroides</i> and <i>Chlorofelxus aurantiacus</i> . By M. Becker, D. Middendorf, N.W. Woodbury, W.W. Parson, and R.E. Blankenship (With 4 Figures)	374
Femtosecond Spectroscopy of the Primary Events of Bacterial Photosynthesis By W. Zinth, J. Dobler, and W. Kaiser (With 3 Figures)	379
An Accumulated Photon Echo Study of Sub-picosecond Processes in Photosynthetic Reaction Centers By S.R. Meech, A.J. Hoff, and D.A. Wiersma (With 2 Figures)	384

Ultrafast Electron and Energy Transfer in Reaction Center and Antenna Proteins from Photosynthetic Bacteria By M.R. Wasielewski, D.M. Tiede, and H.A. Frank (With 5 Figures)	388
Femtosecond Spectroscopy of Excitation Energy Transfer and Initial Charge Separation in the Reaction Center of the Photosynthetic Bacterium <i>Rhodospseudomonas sphaeroides</i> By J. Breton, J.-L. Martin, A. Migus, A. Antonetti, and A. Orszag (With 4 Figures)	393
Picosecond Transient Absorption Spectroscopy of Green Plant Photosystem I Reaction Centres By B.L. Gore, L.B. Giorgi, and G. Porter (With 1 Figure)	398
Femtosecond-Pulse Spectroscopy of Primary Photoprocesses in Reaction Centers of <i>Rhodospseudomonas sphaeroides</i> R-26 By S.V. Chekalin, Yu.A. Matveets, and A.P. Yartsev (With 3 Figures)	402
Detergent Effects upon the Picosecond Dynamics of Higher Plant Light Harvesting Chlorophyll Complex (LHC). By J.P. Ide, D.R. Klug, W. Kuhlbrandt, G. Porter, and J. Barber (With 1 Figure)	406
Picosecond Conformational Intermediates in the Bacteriorhodopsin Photocycle. By G.H. Atkinson, T.L. Brack, D. Blanchard, G. Rumbles, and L. Siemankowski (With 3 Figures)	409
Electron Transfer and Rapid Restricted Motion in Homologous Azurins. By J.W. Petrich, J.W. Longworth, and G.R. Fleming (With 3 Figures)	413
Primary Process of Vision: Hypsorhodopsin By T. Kobayashi, H. Ohtani, and M. Tsuda (With 3 Figures)	416
Reactivity and Dynamics of Hemeproteins in the Femtosecond and Picosecond Time Domains. By D. Houde, J.W. Petrich, O.L. Rojas, C. Poyart, A. Antonetti, and J.L. Martin (With 3 Figures)	419
Picosecond Raman Hole Burning as a Probe of Conformational Heterogeneity: Applications to Oxyhemoglobin By B.F. Campbell and J.M. Friedman (With 4 Figures)	423
Ultrafast Studies of Nitrosylmyoglobin. By K.A. Jongeward, J.C. Marsters, and D. Magde (With 4 Figures)	427
Molecular Dynamics Study of Vibrational Cooling in Optically Excited Hemeproteins. By E.R. Henry, W.A. Eaton, and R.M. Hochstrasser (With 1 Figure)	430

Chemical Reaction in a Glassy Matrix: Dynamics of Ligand Binding to Protoheme in Glycerol:Water. By J.R. Hill, M.J. Cote, D.D. Dlott, J.F. Kauffman, J.D. McDonald, P.J. Steinbach, J.R. Berendzen, and H. Frauenfelder (With 3 Figures)	433
--	-----

Part VIII Energy Transfer and Relaxation

Energy and Electron Transfer of Adsorbed Dyes on Molecular Single Crystals and Other Substrates. By K. Kemnitz, N. Nakashima, and K. Yoshihara (With 5 Figures)	438
Optical Pump-Probe Spectroscopy of Dyes on Surfaces: Ground-State Recovery of Rhodamine 640 on ZnO and Fused Silica By P.A. Anfinrud, T.P. Causgrove, and W.S. Struve (With 1 Figure)	442
Picosecond Fluorescence Spectroscopy on Molecular Association in Langmuir-Blodgett Films By I. Yamazaki, N. Tamai, and T. Yamazaki (With 3 Figures)	444
Fluorescence Concentration Depolarization of DODCI in Glycerol: A Photon-Counting Test of Three-Dimensional Excitation Transport Theory By D.E. Hart, P.A. Anfinrud, and W.S. Struve (With 1 Figure) ...	447
Fractal Behaviors in Two-Dimensional Excitation Energy Transfer on Vesicle Surfaces. By N. Tamai, T. Yamazaki, I. Yamazaki, and N. Mataga (With 3 Figures)	449
Transient Vibrational Heating of Molecules After Internal Conversion. By A. Seilmeier, U. Sukowski, W. Kaiser, and S.F. Fischer (With 2 Figures)	454
Nonlinear Absorption Spectroscopy of Liquids with Ultrashort IR Pulses By H. Graener, R. Dohlus, and A. Laubereau (With 2 Figures)	458
Femtosecond Relaxation Dynamics of Large Organic Molecules By M.J. Rosker, F.W. Wise, C.L. Tang, and A.J. Taylor (With 4 Figures)	461
Population Lifetimes of OH($\nu=1$) and OD($\nu=1$) Vibrations in Alcohols, Silanols and Crystalline Micels. By E.J. Heilweil, M.P. Casassa, R.R. Cavanagh, and J.C. Stephenson	465
S_0 - S_n Two-Photon Absorption Dynamics of Rhodamine Dyes By P. Sperber, M. Weidner, and A. Penzkofer (With 3 Figures)	469

Nonlinear Optical Response of One-Dimensional Excitons in Polydiacetylene. By B.I. Greene, J. Orenstein, R.R. Millard, and L.R. Williams (With 2 Figures)	472
Picosecond Photoconductivity and Nonlinear Optical Phenomena in <i>trans</i> -Polyacetylene By D. Moses, M. Sinclair, and A.J. Heeger (With 1 Figure)	475
Singlet Exciton Fusion in Molecular Solids By R.R. Millard and B.I. Greene (With 2 Figures)	478
Matrix Effect on Vibrational Relaxation in Molecular Crystals By J.R. Hill, E.L. Chronister, J.C. Postlewaite, and D.D. Dlott (With 1 Figure)	482
Optical Damage in Molecular Crystals: A Solid State Explosion By D.D. Dlott, T.J. Kosic, and J.R. Hill (With 4 Figures)	485
Rotational Relaxation of Free and Solvated Rotors By A.J. Bain, C. Han, P.L. Holt, P.J. McCarthy, A.B. Myers, M.A. Pereira, and R.M. Hochstrasser (With 5 Figures)	489
Ultrafast Dynamics at the Interface: Probing the Transition from Solution to Surface Interactions in Charged Micelles By E.F. Templeton, K. Brinker, S. Paone, and G.A. Kenney-Wallace (With 1 Figure)	495
Shock Moderated Photophysics and Photochemistry at Multi-kilobar Pressures By B.L. Justus, A.L. Huston, and A.J. Campillo (With 5 Figures) .	499

Part IX Coherent Spectroscopic Techniques

Phase Grating Approach to Susceptibility Tensors: Determination in Isotropic Media. By J. Etchepare, G. Grillon, I. Thomazeau, G. Hamoniaux, and A. Orszag (With 4 Figures)	504
Nonlinear Response Function for Four-Wave Mixing: Application to Coherent Raman Lineshapes in Polyatomics and to the Optical Anderson Transition By S. Mukamel, Z. Deng, and R.F. Loring (With 2 Figures)	510
Picosecond Laser Pulse Shaping and Phase Shifting for Molecular Spectroscopy By M. Haner, F. Spano, and W.S. Warren (With 2 Figures)	514
Third-Order Nonlinear Optical Interactions in Thin Films of Organic Polymers Investigated by Picosecond and Subpicosecond Four-Wave Mixing. By P.N. Prasad, D. Narayana Rao, J. Swiatkiewicz, P. Chopra, and S.K. Ghoshal	518

Picosecond Raman-Induced Phase Conjugation Spectroscopy By R. Dorsinville, P. Delfyett, and R.R. Alfano (With 2 Figures) ..	521
Polarization Dependence of Time-Resolved CARS in Liquids By N. Kohles and A. Laubereau (With 3 Figures)	524
Direct Measurement of Wave-Vector-Dependent Polariton Energy Velocity and Dephasing in NH_4Cl By G.M. Gale, F. Vallée, and C. Flytzanis (With 4 Figures)	528
Impulsive Stimulated Rayleigh, Brillouin, and Raman Scattering: Experiments and Theory of Light Scattering Spectroscopy in the Time Domain. By M.R. Farrar, L.R. Williams, Yong-Xin Yan, Lap-Tak Cheng, and K.A. Nelson (With 4 Figures)	532
Ultrafast Transient Spectroscopy with Broadband Non-Transform- Limited Light Sources By T. Yajima and N. Morita (With 4 Figures)	536
Picosecond Dephasing Time Measurement by CSRS Using Temporally Incoherent Nanosecond Laser with Short Correlation Time By T. Kobayashi, T. Hattori, and A. Terasaki (With 3 Figures) ...	541
Anomalous Pulse Duration Dependence of the Quasicontinuum Absorption Spectrum By P. Mukherjee and H.S. Kwok (With 3 Figures)	544
Index of Contributors	549

Femtosecond Spectroscopy of the Primary Events of Bacterial Photosynthesis

W. Zinth, J. Döbler, and W. Kaiser

Physik Department der Technischen Universität München,
Arcisstraße 21, D-8000 München 2, Fed. Rep. of Germany

Recent investigations of bacterial photosynthesis have shown that the primary steps occur on the time scale of one picosecond /1-3/. These processes can only be studied by means of ultrafast optical techniques. The standard experimental methods yield absorption changes induced by a short excitation pulse measured as a function of time and wavelength. Experiments are now possible with the temporal resolution of better than 100 fs. They present interesting information on the early dynamics of the primary processes. Optical techniques alone provide insufficient understanding of the molecular microscopic processes of the primary steps. It is important to add information from other experiments, e.g. from structure analysis, resonance Raman scattering, molecular dynamics calculations or experiments on model compounds.

In this note we are concerned with time-resolved experiments of the primary steps of photosynthetic units such as bacteriorhodopsin and bacterial reaction centers. We combine the results of ultrafast spectroscopy with other available data in order to gain a better insight into the molecular processes of the primary events.

Experimental

The experiments are performed using amplified pulses ($t_p=100$ fs, repetition rate 7.5 kHz) from a colliding pulse mode-locked laser operating at 620 nm for the excitation of the samples. Probing pulses are obtained by continuum generation in a jet of ethylene glycol. A narrow fraction of the continuum ($\Delta\lambda \approx 10-15$ nm) was selected. The probe pulses monitor the absorbance changes of the sample as a function of time delay between exciting and probing pulses. In order to avoid high exposure the sample was kept in a spinning cuvette. In this way, it was ascertained that each photosynthetic unit absorbs one photon only every second. There was no indication of any photodecomposition of the samples at the excitation densities used in the experiments (less than 10% of the molecules absorb one photon per excitation pulse).

Bacteriorhodopsin

Bacteriorhodopsin (BR) is a membrane protein contained in the cell membrane of Halobacterium halobium. It acts as a light-driven proton pump building up a proton gradient across the cell membrane upon illumination.

The absorption properties of BR are determined by the only pigment molecule retinal. Retinal is bound in BR via a Schiff base to one lysine of the polypeptide chain. In the light-adapted form of BR, the retinal molecule has the all-trans configuration and the Schiff base is protonated. During the photochemical cycle the absorption properties of BR change substantially. Intermediate states named J,K,L,M,... have been

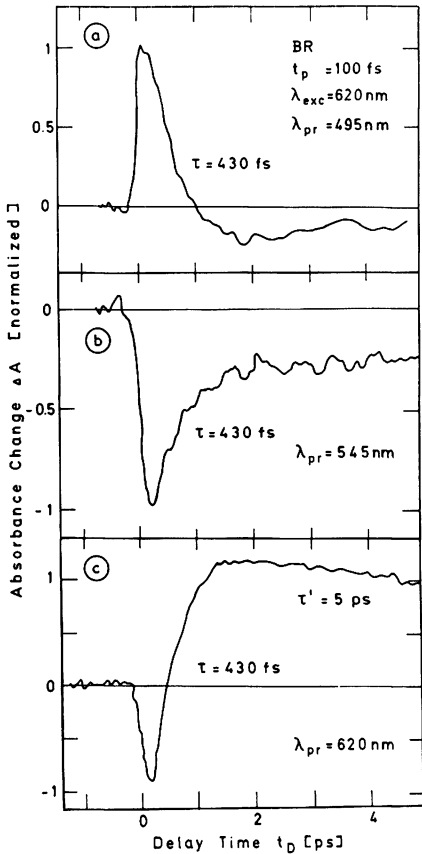


Fig.1 Bacteriorhodopsin: Absorption changes induced by 100 fs excitation pulses at 620 nm

identified. During the course of the cycle the retinal adopts the 13-cis configuration and the Schiff base loses its proton. The photochemical cycle is completed after ~ 10 ms. The first events of the photocycle of BR, where the optical energy is stored in the molecules, have been studied in a number of publications. It was not until recently, that a coherent picture of the primary molecular process was presented /1,4,5/.

Fig.1 shows absorption changes measured as a function of time delay after excitation of the BR molecules at 620 nm. When the molecules are probed at 490 nm, a strong induced absorption is found which builds up with the time resolution of the experiment of 100 fs. In a first relaxation process this absorption change decays with a time constant of 430 fs into a state of reduced absorption from which a slow 5 ps kinetic leads to a partial recovery of the absorption, which stays constant for times longer than 12 ps (not shown in Fig.1). The same time constants (< 100 fs, 430 fs, and 5 ps) are found at the other probing wavelengths of 545 nm and 620 nm in Fig.1b and c, respectively.

The results presented above together with additional information from femtosecond experiments on deuterated BR /1/, from picosecond data on BR containing a sterically fixed retinal molecule /6/, and from resonance Raman

scattering /7/ yield the following microscopic picture of the primary molecular processes: Light promotes BR to a Franck-Condon state on the excited-state potential surface. From there a very fast ($\tau < 100$ fs) molecular motion leads to the bottom of the S_1 potential surface. Internal conversion with $\tau' = 430$ fs leads to the ground state intermediate J which contains the isomerized 13-cis retinal. Rearrangements of the protein surrounding causes the slower 5 ps kinetics leading to the intermediate K which is stable for the longer time of 300 ps.

Reaction Centers

Photosynthesis in green plants and in most bacterial systems uses chlorophyll or bacteriochlorophyll molecules arranged in so-called reaction centers (RC) where a primary charge separation is initiated. Reaction centers can be isolated from some bacteria. The reaction centers of Rhodospseudomonas viridis or Rhodospseudomonas spheroides contain six pigments absorbing in the visible and near infrared: 4 bacteriochlorophyll (BChl) and 2 bacteriopheophytin (BPh) of type b and a for R-viridis and R-spheroides, respectively. Two of the BChl form the excitonically coupled special pair, from which the charge separation originates. A major progress in the understanding of the molecular processes in the RC was recently achieved when the reaction centers of R-viridis were crystallized /8/ and when a structural analysis of these RC was completed /9/. The arrangement of pigments obtained by structure analysis allowed calculation of the excitonic coupling: it was shown that there is strong excitonic mixing between the various pigments of the RC, substantially influencing the absorption in the near infrared spectral region ($\lambda > 750$ nm) /10/.

It is the purpose of this chapter to compare the dynamic absorption changes in R-viridis - where the pigment arrangement is known - with those of R-spheroides. In addition, the data give information on excitation transfer between the pigments in the RC. Because of the strong excitonic interaction which influences the IR absorption bands we concentrate here on the visible absorption where the Q_x transitions are located. BChl absorbs around 600 nm, BPh around 540 nm and - in the RC of R-viridis - the special pair (P) exhibits a shoulder in the absorption around 620 nm.

Time-resolved absorption measurements are shown in Fig.2 for R-viridis (a,b) and R-spheroides (c,d) after excitation at 620 nm. First we probed around 545 nm at a frequency where the BPh absorbs. The data show at later delay times, i.e. for $t_D > 200$ fs a decay of the absorption with a time constant of 2.8 ps for both types of RC. The absorption decreases at 545 nm, where initially the BPh's absorb strongly suggesting that BPh is reduced to form BPh^- . Additional experiments at $\lambda = 675$ nm, a wavelength where BPh^- absorbs, support this interpretation. Figs. 2b and d show the rise of the absorption change on an expanded scale. In both cases the rise follows closely the integrated cross-correlation curve between exciting and probing pulses. We may deduce from these data that the absorption appears within our time resolution of 100 fs for the RC of R-viridis and R-spheroides. The molecular nature of this early state requires some consideration. It may simply be the excited electronic state P^* of the special pair or it is a state P^{*-} which contains considerable contribution from a charge transfer state /2/. Both interpretations are possible within the scope of present knowledge.

The experimental findings of the two time constants of < 100 fs and 2.8 ps allow us to draw the following conclusions: After absorption of a photon at 620 nm the excitation is rapidly transferred, $\tau < 100$ fs, to

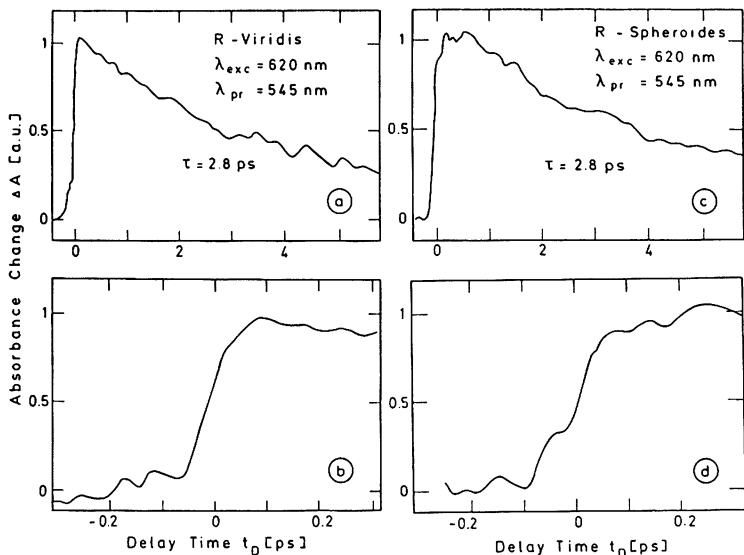


Fig.2 Reactions centers: Transient absorption changes measured at the probing wavelength 545 nm, where initially the BPh absorb. The same time dependence is found for the formation of BPh⁻ in the two reaction centers.

the special pair to form the primary state P* or P⁺-. Subsequently, reduction of BPh to BPh⁻ occurs within 2.8 ps. Since both systems, the RC of R-viridis and of R-spheroides, behave in the same manner, we believe that their pigment arrangements and the interactions between the pigments are very similar.

Conclusions

The present investigations of the bacterial photosynthesis of two very different photosynthetic systems - bacteriorhodopsin and bacterial reaction centers - suggest very high reaction rates of the primary events. This common property can be well understood with the help of the reaction scheme shown in Fig.3. After optical excitation, fast molecular rearrangements occur on the excited-state potential surface. From there two pathways are possible: internal conversion to the initial ground

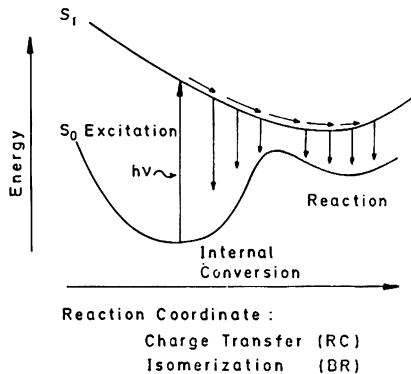


Fig.3 Schematic of the energy surfaces indicating the primary reactions in the investigated photosynthetic systems

state and the desired photochemical reaction. The internal conversion rates for most large pigment systems are very rapid. For this reason, the reactive channel must be faster in order to maintain reasonable quantum efficiencies in the first photosynthetic steps.

Acknowledgement

The authors gratefully acknowledge valuable contributions from H. Michel, D. Oesterhelt, and H. Scheer.

- 1 M.C. Nuss, W. Zinth, W. Kaiser, E. Kölling, D. Oesterhelt, *Chem. Phys. Lett.* 117 (1985) 1
- 2 J.-L. Martin, J. Breton, A. J. Hoff, A. Migus, A. Antonetti, *Proc. Nat. Acad. Sci. USA* 83 (1986) 957
- 3 W. Zinth, M.C. Nuss, M.A. Franz, W. Kaiser, H. Michel, in "Antennas and Reaction Centers of Photosynthetic Bacteria", ed. M.E. Michel-Beyerle, Springer, Berlin 1985, p.286
- 4 H.J. Polland, M.A. Franz, W. Zinth, W. Kaiser, E. Kölling, D. Oesterhelt, *Biophys. J.* 49 (1986) 651; H.J. Polland, W. Zinth, W. Kaiser, in "Ultrafast Phenomena IV", ed. D.H. Auston, K.B. Eisenthal, Springer Series in Chem. Phys., Springer, Heidelberg 1984, p. 456
- 5 A.V. Sharkov, A.V. Pakulev, S.V. Chekalin, Y.A. Matveetz, *Biochim. Biophys. Acta* 808 (1985) 94
- 6 H.J. Polland, M.A. Franz, W. Zinth, W. Kaiser, E. Kölling, D. Oesterhelt, *Biochim. Biophys. Acta* 767 (1984) 635
- 7 M. Braiman, R. Mathies, *Proc. Nat. Acad. Sci. USA* 79 (1982) 403
- 8 H. Michel, *J. Mol. Biol.* 158 (1982) 567
- 9 J. Deisenhofer, O. Epp, K. Miki, R. Huber, H. Michel, *J. Mol. Biol.* 180 (1984) 385
- 10 W. Zinth, E.W. Knapp, S.F. Fischer, W. Kaiser, J. Deisenhofer, H. Michel, *Chem. Phys. Lett.* 119 (1985) 1